Saha, S., U. Greferath, K. A. Vessey, D. B. Grayden, A. N. Burkitt, and E. L. Fletcher. 2016. Changes in ganglion cells during retinal degeneration. *Neuroscience*. **329**: 1-11.

doi: https://doi.org/10.1016/j.neuroscience.2016.04.032

Please cite this article in press as: Saha S et al. Changes in ganglion cells during retinal degeneration☆. Neuroscience (2016), http://dx.doi.org/10.1016/j.neuroscience.2016.04.032

Neuroscience xxx (2016) xxx–xxx

CHANGES IN GANGLION CELLS DURING RETINAL DEGENERATION☆

SUSMITA SAHA,[a,b,c] URSULA GREFERATH,[a] KIRSTAN A. VESSEY,[a] DAVID B. GRAYDEN,[b,c,d,e] ANTHONY N. BURKITT[b,c,d,e] AND ERICA L FLETCHER[a]*

[a] *Department of Anatomy and Neuroscience, The University of Melbourne, Australia*

[b] *NeuroEngineering Laboratory, Department of Electrical & Electronic Engineering, The University of Melbourne, Australia*

[c] *Centre for Neural Engineering, The University of Melbourne, Australia*

[d] *NICTA Victoria Research Laboratory, c/- Dept. of Electrical & Electronic Engineering, The University of Melbourne, Australia*

[e] *Bionics Institute, East Melbourne, Australia*

Abstract—Inherited retinal degeneration such as retinitis pigmentosa (RP) is associated with photoreceptor loss and concomitant morphological and functional changes in the inner retina. It is not known whether these changes are associated with changes in the density and distribution of synaptic inputs to retinal ganglion cells (RGCs). We quantified changes in ganglion cell density in rd1 and age-matched C57BL/6J-(wildtype, WT) mice using the immunocytochemical marker, RBPMS. Our data revealed that following complete loss of photoreceptors, (~3 months of age), there was a reduction in ganglion cell density in the peripheral retina. We next examined changes in synaptic inputs to A type ganglion cells by performing double labeling experiments in mice with the ganglion cell reporter lines, rd1-Thy1 and age-matched wildtype-Thy1. Ribbon synapses were identified by co-labelling with CtBP2 (RIBEYE) and conventional synapses with the clustering molecule, gephyrin. ON RGCs showed a significant reduction in RIBEYE-immunoreactive synapse density while OFF RGCs showed a significant reduction in the gephyrin-immmunoreactive synapse density. Distribution patterns of both synaptic markers across the dendritic trees of RGCs were unchanged. The change in synaptic inputs to RGCs was associated with a reduction in the number of immunolabeled rod bipolar and ON cone bipolar cells. These results suggest that functional changes reported in ganglion cells during retinal degeneration could be attributed to loss of synaptic inputs. © 2016 Published by Elsevier Ltd. on behalf of IBRO.

Key words: ganglion cell, retinitis pigmentosa, plasticity, retina, inner plexiform layer.

INTRODUCTION

Retinitis pigmentosa refers to a family of inherited retinal degenerations caused by the gradual loss of photoreceptors, rods followed by cones, that leads to complete loss of vision. Over recent years there has been a great deal of interest in the efficacy of photoreceptor restorative therapies (Chader et al., 2009; O'Brien et al., 2012). Restoration of vision however, is only possible if retinal ganglion cells, the output neurons of the retina, remain intact and capable of passing visual information to higher brain centers. It is now known that after photoreceptors die there are a myriad of changes that affect inner retinal neurons including ganglion cells (Santos et al., 1997; Humayun et al., 1999; Strettoi and Pignatelli, 2000; Strettoi et al., 2002, 2003; Marc et al., 2003). Notably, functional changes in RGCs have been reported during the early stages of degeneration manifesting as an increased oscillatory spontaneous spike activity [RCS rat (Pu et al., 2006), rd1 and rd10 mice (Margolis et al., 2008; Stasheff, 2008; Stasheff et al., 2011) and P23H rat (Sekirnjak et al., 2011)]. This aberrant ganglion cell activity may explain the unusual photopsia that patients with retinitis pigmentosa experience and that significantly affects quality of life. The underlying factors that contribute to alterations in RGC function during retinal degeneration remain to be determined.

The functional output, or excitability, of neurons is determined by the balance of excitatory and inhibitory inputs. In healthy mammalian retinae, ganglion cells receive glutamatergic (excitatory) synaptic inputs from at least ten different cone bipolar cells via ribbon synapses (Wässle et al., 2009). Inhibitory input to ganglion cells is formed from a variety of predominantly GABAergic or glycinergic amacrine cells that communicate with ganglion cells at conventional synapses. The distribution of excitatory synapses across ganglion cell dendrites is largely uniform across a number of ganglion cell types and species (Jakobs et al., 2008; Xu et al., 2008; Koizumi et al., 2011; Chen and Chiao, 2014). However, the balance of excitatory to inhibitory synaptic inputs varies across different ganglion cell types (Freed and Sterling, 1988; Erikoz et al., 2008; Percival et al., 2009, 2011, 2013), across different species and also during development (Soto et al., 2011). The effect of disease on the spatial distribution of excitatory and inhibitory inputs to ganglion cells is not known. It is possible that with

☆ This work was supported by the NHMRC project grant (APP1021042), by Retina Australia, and the Australian Research Council, through its Special Research Initiative in Bionic Vision Science and Technology grant to Bionic Vision Australia.

*Corresponding author. Address: Department of Anatomy and Neuroscience, The University of Melbourne, Grattan Street, Parkville 3010, Victoria, Australia. Tel: +61-3-8344-3218; fax: +61-3-9347-521.

E-mail address: elf@unimelb.edu.au (E. L Fletcher).

Abbreviations: ANOVA, analysis of variances; RG_A, A-type RGCs; RGCs, retinal ganglion cells; RP, retinitis pigmentosa.

http://dx.doi.org/10.1016/j.neuroscience.2016.04.032
0306-4522/

remodeling events that take place within the inner retina during retinal degeneration, that changes in the spatial distribution of synapses develop, leading to functional changes in these cells.

All bipolar cell inputs to ganglion cells occur at ribbon synapses and therefore it is possible to quantify the distribution of synaptic inputs to ganglion cells using immunocytochemical labelling of ribbon-associated proteins such as CtBP2 (RIBEYE; (Schmitz et al., 2000; Percival et al., 2011). Quantification of the spatial distribution of inhibitory synapses is possible using immunolabeling of the post-synaptic anchoring protein, gephyrin. Gephyrin is known to tether all glycine receptors as well as $GABA_A$ receptors containing α1, α2 and α3 subunits to the cytoskeleton (Tyagarajan and Fritschy, 2014), receptor types that are known to be expressed by retinal ganglion cells (Koulen et al., 1996). For example, gephyrin has been used previously to identify inhibitory synaptic inputs to midget and parasol ganglion cells of the primate retina (Percival et al., 2009, 2011). Using these markers of excitatory and inhibitory synaptic inputs it is possible to determine whether the reported functional changes in ganglion cells in retinal degeneration are a result of altered input to ganglion cells, intrinsic changes in ganglion cells or a combination of both.

The aim of this study was to characterize ganglion cell changes in the rd1 retina. We first evaluate the density of ganglion cells using the ganglion cell marker, RBPMS and then compared the density and distribution of excitatory and inhibitory synapses on A type ON- and OFF-RGCs in wildtype and rd1 mice. Overall, our results show that ganglion cells are reduced in density in the peripheral retina after photoreceptor loss. In addition, ON RGCs were associated with a reduced density of excitatory synapses, while OFF RGCs were associated with a reduced density of inhibitory synapses. Moreover, there was a reduction in the density of ON cone and rod bipolar cells. These results highlight that following photoreceptor loss, there are significant changes in synaptic inputs and also in ganglion cell integrity. The shifts in excitatory and inhibitory inputs observed could partially explain the functional changes observed in ganglion cells during retinal degeneration.

EXPERIMENTAL PROCEDURES

Animals

All animal procedures and protocols were approved by the University of Melbourne Animal Experimentation Ethics Committee and were performed according to the guidelines outlined by the National Health and Medical Research Council and the ARVO Statement for the Use of Animals in Ophthalmic and Vision Research.

Rd1-Thy1-Yellow Fluorescent Protein (YFP) mice were developed by crossing rd1 with Thy1-YFP mice. The rd1 mouse model was originally obtained from Professor Debora Farber (University of California, Los Angeles, USA) and Thy1-YFP homozygous mice (Line M described by Feng et al. (2000)) was kindly donated by Professor Anthony Hannan (Howard Florey Institute, Parkville, VIC). All mouse strains were on a C57B6J background, and were confirmed by genotyping to be free of the $rd8^{Crb1/Crb1}$ mutation. In this study, a total of 18 rd1-Thy1 mice aged 1 month and 34 rd1-Thy1 aged 3 months were investigated. Homozygous Thy1 mice were controls (1 month, $n = 16$ mice; 3 months: $n = 24$ mice).

Immunocytochemistry

Mice were killed by cervical dislocation, their eyes removed immediately, the anterior contents dissected and the posterior eyecups placed in 4% paraformaldehyde for 30 min. Posterior eyecups were then processed for indirect immunofluorescence as previously described (Fletcher, 2000; Ho et al., 2012; Vessey and Fletcher, 2012). Briefly, posterior eyecups were processed through graded sucrose solutions (10%, 20% sucrose (w/v) in 0.1 M phosphate buffer, pH 7.4 (PB)) followed by 30% sucrose overnight. The next day, the tissues were frozen in liquid nitrogen and subsequently frozen and thawed three times to enhance antibody penetration. Tissues were washed with 0.1 M PB and preincubated in a solution containing 0.5% Triton + 0.5% DMSO in PB for 1 h.

Excitatory synaptic ribbons were identified by labeling with mouse anti-CtBP2 (RIBEYE; 1:2000) (BD Transduction Laboratories, Cat#612044), a marker for excitatory, ribbon synapses (Schmitz et al., 2000; Vessey and Fletcher, 2012). Inhibitory, conventional synapses were identified by immunolabeling with mouse anti-gephyrin (1:500) (Synaptic Systems, Germany; Cat #147011, (Haverkamp and Wässle, 2000)). Glycine receptors and $GABA_A$ receptors containing the α1, α12 and α13 subunits are known to be tethered to the cytoskeleton by gephyrin (Tyagarajan and Fritschy, 2014). Rod bipolar cells were immunolabeled with a monoclonal mouse antibody against protein Kinase Cα (diluted 1:400; Clone #P5704, Sigma, Missouri, USA) (Greferath et al., 1990). ON-cone bipolar cells (ON-CBCs) were identified by double labeling of PKC and Goα (1:500; rabbit anti-Goα; Millipore (Vardi, 1998)) and quantifying all Goα bipolar cells that were protein kinase C negative. OFF cone bipolar cells were immunolabeled with mouse anti-ZNP-1 (synaptotagmin 2; 1:2000 Clone #ZDB-ATB-081002-25, ZIRC, Eugene Oregon, USA) which has been shown previously to immunolabel type 2 and type 6 bipolar cells in the mouse retina (Wässle et al., 2009). For quantification of ganglion cells, flat-mounted retinae were immunolabeled for RNA-binding protein with multiple splicing, RBPMS, a marker of ganglion cells in the mouse retina (Rodriguez et al., 2014), using a rabbit anti-RBPMS (1:250, Abcam, Cat #ab194213). Retinal flatmounts were incubated in primary antisera for 3 days at room temperature and were then incubated in secondary antibody for 1 day at 4 °C. Following further washing in 0.1 M PB, retinal flatmounts were mounted on slides and cover slipped in mounting medium (DAKO, Carpinteria, USA).

Some retinae were sectioned transversely at 14 μm using a cryostat. Vertical sections of retinae were processed for immunostaining as follows. Tissue sections were incubated in 1% normal goat serum, 0.5%, Triton-X100 and 0.05% Sodium Azide in

Please cite this article in press as: Saha S et al. Changes in ganglion cells during retinal degeneration☆. Neuroscience (2016), http://dx.doi.org/10.1016/j.neuroscience.2016.04.032

0.1 M PB, with the corresponding primary antibodies overnight. Sections were then washed and incubated for 1 h with the corresponding secondary antibody conjugated to Goat anti-mouse conjugated to AlexaFluor 594 (Invitrogen, VIC, Australia; diluted 1:500) or Goat anti-GFP-488, which cross reacts with the Thy1-YFP tag (Diluted 1:400, Rockland Immunochemicals, Gilbertsville, PA, USA). Finally, they were mounted on slides with the mounting medium (Dako Fluorescence Mounting Medium, Carpinteria, USA).

Microscopy and imaging

Immunolabeled specimens were viewed on a confocal laser-scanning microscope (LSM 510, PASCAL, Zeiss, Oberkochen, Germany) using a PlanApo x63 1.4NA objective. Excitation was provided by 488-nm and 561-nm lasers with emission being captured with 504–569-nm filters for the green channel and 591–719 nm for the red channel. For flat-mounted retinae labeled with PKCα and ZNP-1, confocal Z-stacks were collected using a $\times$40 oil objective at 1-μm optical sections through the inner nuclear and plexiform layers using Zeiss Zen software. Images were imported into the computer software Imaris ($\times$64, v.7.7.0 Bitplane AG, Zürich, Switzerland) for analysis and 5–10 microns of the cell bodies in the nuclear layer and also the corresponding dendrites in the inner plexiform layer were selected and presented as three dimensional projections using the *Surpass mode*.

Imaging of dendritic fields of ganglion cells was achieved in two ways. First, the entire dendritic field was captured by tiling 3 $\times$ 3 images of A-ON and A-OFF cells at 63$\times$ magnification. Second, to reduce the time needed for capture, some images covered only half the dendritic field. To satisfy the Nyquist-Shannon sampling criterion, an X–Y pixel size of 0.13 μm and a z-step size of 0.17 μm were used for imaging. We verified that the synaptic density quantified across ON and OFF ganglion cells was no different regardless of the imaging procedure used by comparing synaptic density across the entire dendritic tree with the synaptic density across a partial dendritic field for the same cell. The densities of excitatory and inhibitory synapses were similar for methods of analysis (n = 15 cells; paired t-test, $P < 0.0001$, correlation coefficient = 0.9983). In this study, data were collected from a total of 181 cells from 3 to 12 mice retinae per age group per strain.

Image analysis

Morphological characteristics of ON and OFF RG_A retinal ganglion cells. In both Rd-Thy1 and wiltype-Thy1 mice, the thy-1-YFP tag labeled a range of distinct ganglion cell types across the flatmounted retina (Fig. 1A). In our study, A-type RGCs (RG_A) were identified based on morphological characteristics including soma size, dendritic field size and the radiating pattern of branching, as previously described by Sun et al. (2002); Fig. 1B, C). In order to quantify dendritic field area we manually connected the distal tips of dendrites to form a polygon (Fig. 1B). Soma diameter was measured by connecting boundary points on the circumference of the soma (Fig. 1C). Then, we calculated the area of the polygon and, for simplification, considered it as a circle. Finally, the radius of the circle was measured from the equation: πr^2 = area where r is the radius and diameter was calculated from 2*r. In our study, RG_A cells had a soma diameter range of 16–29.73 μm and dendritic field diameter ranging from 123.16 to 463.18 μm.

Dendritic arbors of ON and OFF ganglion cells stratify in different depths within the IPL in wildtype retinae (Famiglietti and Kolb, 1976). Using Z-stack confocal images, the stratification of ganglion cell dendritic arbors was calculated based on percentage depth of the inner plexiform layer where ganglion cell arbors were located. Ganglion cells in both wildtype and rd1 retinae were identified as ON cells if they stratified within 0–40% of the IPL depth and as OFF cells if they stratified within 60–100%. Following identification of the RGC type, dendritic length and area were measured using MetaMorph software (Angiogenesis Tube formation Module; Molecular Devices, Sunnyvale, CA, USA).

Quantification of synaptic density. We examined whether there were changes in synaptic inputs into A type ganglion cells of the rd1 retina compared to controls by performing double labeling experiments on retinae from Thy1-YFP and rd1-Thy1 mice aged 1 and 3 months of age using RIBEYE as a marker of excitatory, ribbon synapses and gephyrin as a marker of conventional, inhibitory synapses. The density of synapses was analyzed by quantifying the number of co-localized puncta over an entire dendritic tree, or across a partial dendritic tree.

Excitatory and inhibitory synapses were extracted using a Top Hat filter and image segmentation to generate a binary mask in Metamorph. This mask was then used to extract only the puncta that were in contact with labeled dendrites. For any puncta to be considered co-localized with a dendrite, the binarised puncta had to overlap with a fixed intensity value of the dendrite. The intensity cut-off was determined by the full width half maximum of the dendritic stain intensity/edge. We measured the puncta density in both puncta per 100 μm^2 of dendritic membrane as well as puncta per linear μm of dendrite.

We developed an automated method for the quantification of colocalized puncta on dendrites using an iterative approach. Briefly, we compared the number of puncta associated with a dendrite as determined by an automated method with results generated from a manual determination method and then modified our automated script until the automatic method was compatible with our manual observations. However, a limitation of using confocal microscopy rather than ultrastructural analysis for the determination of synaptic inputs to dendrites is the potential for overestimation because of blur in the confocal images. To correct for false-positive puncta we introduced three correction factors. First, we discarded the synapses between rod bipolar cells and ganglion cells from our analysis,

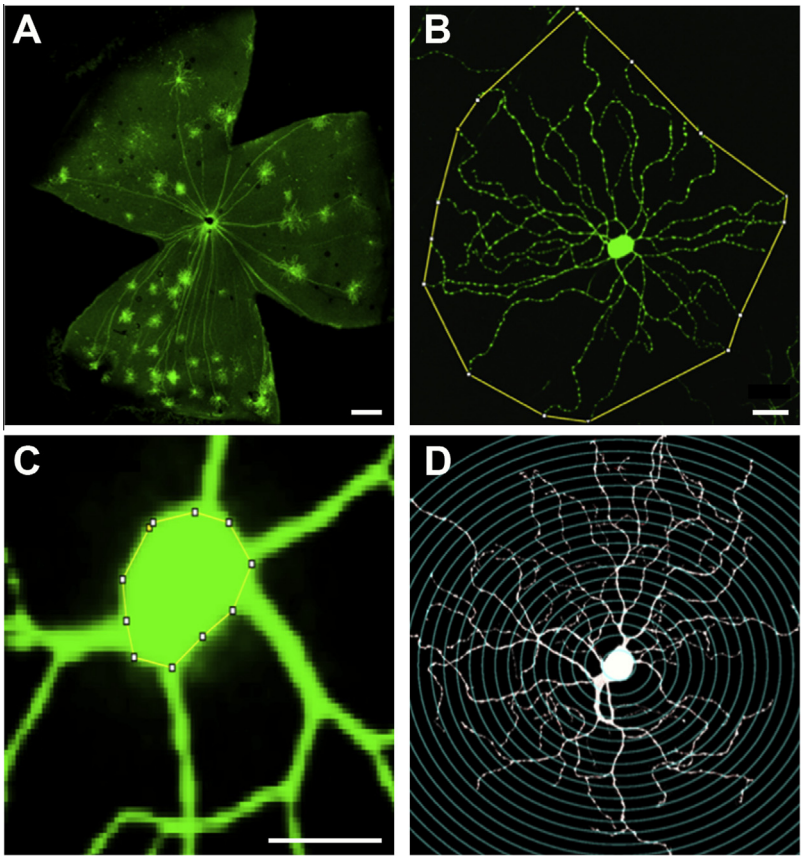

Fig. 1. (A) Flatmounted Thy1 retina labeled for GFP showing ~ 50 ganglion cells of various types across the retina. (B) Higher magnification of an A type ganglion cell showing dendritic field diameter measurement. (C) Soma diameter measurement by drawing a polygon (yellow line) connecting the boundary tips of the soma. (D) Analysis of synapse distribution by setting the annulus across the dendritic field of a cell. Images were produced using Metamorph, after analysis. Scale bar, 50 μm. (For interpretation of the references to colour in this figure legend, the reader is referred to the web version of this article.)

because these two types of cells are known to have no synaptic contacts (Wässle et al., 1991). To do this we performed triple labeling experiments with RIBEYE, PKCα and GFP labeled dendrites. The percentage of false positives is:

$$\frac{\text{Number of false postive puncta}}{\text{Total number of puncta associated with the dendrites of ganglion cells}} \times 100$$

The average correction factor was 29%. Secondly, we tested whether the number of contacts differed from the number expected by chance. We rotated a dendritic tree around an axis parallel to the retinal surface and quantified the number of puncta associated with this "flipped" dendrite. The number of apparent synaptic contacts significantly reduced to about ~15% (10 cells, Wilcoxon sign-rank test, $P < 0.01$). As a final control, we analyzed the extent of colocalization of RIBEYE and gephyrin with somata ($n = 5$ cells) and the average correction factor was 7.4%.

$$\frac{\text{Number of puncta associated with soma}}{\text{Number of puncta associated with the total cell}} \times 100$$

The maximum false positive rate of 29% was then used as the final correction factor (FCF) to calculate the actual density of synapses on the ganglion cells:

$$\frac{\text{Number of puncta associated with a RGC} - \text{number of false positive puncta}}{\text{denditic area } (\mu m^2) \text{of that cell}} \times 100$$

Distribution of synaptic inputs across the RGC dendritic tree. We quantified the change in synaptic density across RGC dendritic fields by applying a series of concentric rings around the cell body and determined density within each ring in puncta/linear μm of dendrite. The center of a cell's soma was defined as the centroid and masks were created at 10- μm steps from the centroid (Fig. 1D).

Quantification of ganglion cell and bipolar cell density. The density of ganglion cells was quantified in flat-mounted wildtype and rd1 retinae aged 3 months that had been immunolabeled for RBPMS. Using a ×20 air objective, confocal Z-stacks were taken through the RGC layer in three regions in both central and peripheral retina of $n = 5$ wildtype and $n = 5$ rd1 retinae. For quantification of RGC number, images were bandpass filtered and counted using the Image-based Tool for Counting Nuclei (ITCN) macro available in ImageJ (1.43, NIH, USA). Cell counts are presented as number of cells per area (mm^2) of retina.

The density of immunolabeled rod bipolar cells and ON-cone bipolar cells was quantified in transverse retinae labeled with PKC and Goα by counting the number of PKC-immunoreactive somata and Goα-positive, PKC-immunonegative somata in three consecutive sections from the central and peripheral retina. We measured the area of the INL in Metamorph with a free region selection tool. Cell density was measured in cells/mm^2.

Statistical analysis

Data were represented as mean ± SEM. Student's *t*-test or two-way analysis of variances (ANOVA) were used to test excitatory and inhibitory synaptic inputs to RGCs in degenerate (rd1-Thy1) and wildtype (Thy1) mice at different ages (1 months, 3 months) where appropriate. For the two-way ANOVA, where there were significant interaction terms, Tukey's tests were used as post hoc pairwise comparisons to evaluate the differences between diseases at each age, Statistical analysis was performed using GraphPad Prism (v5, GraphPad Software, San Diego, CA). In all figures, statistical significance is expressed as $^{*}P < 0.05$.

RESULTS

The number of ganglion cells is reduced in the peripheral retina of three-month-old rd1 mice

The density of ganglion cells across the retina was assessed in three-month-old rd1 and wildtype mice by immunolabelling retinal wholemounts with the ganglion cell marker, RBPMS. As shown in Fig. 2, RBPMS is a robust marker of ganglion cells in both wildtype (Fig. 2A, WT) and rd1 retinae (Fig. 2B). Quantification of ganglion cell density in the rd1 and control retinae revealed a global reduction in ganglion cell density that could be primarily attributed to loss of ganglion cells in the peripheral retina of the 3-month-old rd1 retina (Fig. 2C; Student's *t*-test, $p < 0.05$).

Changes in excitatory and inhibitory synapses associated with ON ganglion cells during degeneration

ON and OFF A-type ganglion cells were identified in rd1-Thy1 mice and Thy1 controls by the stratification pattern of their dendrites (Fig. 3). No difference in dendritic length was observed in A-type ON or OFF ganglion cells in wildtype-Thy1 compared to rd1-Thy1 retinae at 3 months of age (data not shown) consistent with previous studies (Damiani et al., 2012; Lin and Peng, 2013; O'Brien et al., 2014).

As shown in Fig. 4, many small RIBEYE (red, Fig. 4A) and gephyrin- (red, Fig. 4C) immunoreactive puncta were visible associated with the dendrites of A type ganglion cells (green). Quantification of the number of RIBEYE (Fig. 4B) and gephyrin- (Fig. 4D) immunoreactive puncta associated with ON A-ganglion cell processes revealed that there were a greater number of RIBEYE-immunoreactive (excitatory) puncta associated with ON A-ganglion cell processes than gephyrin-immunoreactive (inhibitory) puncta ($p < 0.05$) in the wildtype retina (Fig. 4E, WT). In contrast, there was no difference in the number of RIBEYE- and gephyrin-immunoreactive

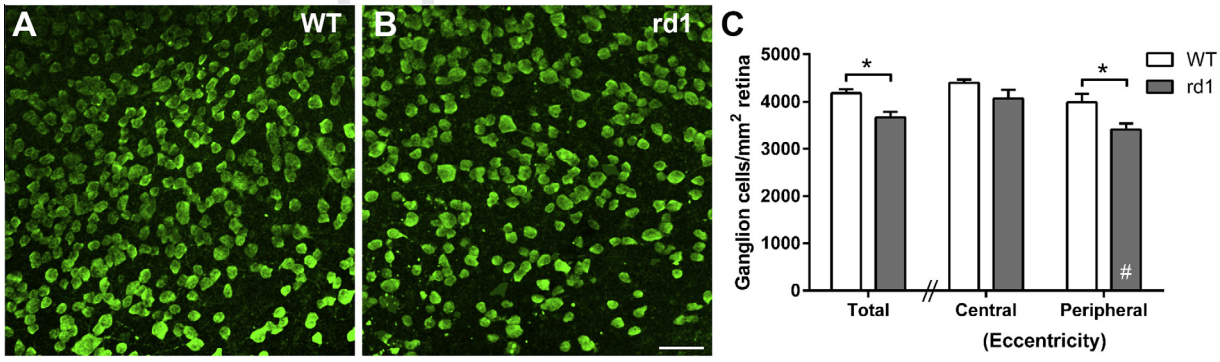

Fig. 2. Ganglion cell density in control and rd1 retinae. Flatmount control (A) and rd1 (B) retinae immunolabeled for the ganglion cell marker, RBPMS. In the periphery, there appear to be fewer ganglion cells in the rd1 retina compared to controls. (C) Graph showing mean ± SEM density of RBPMS-immunoreactive ganglion cells in the wildtype and rd1 retina aged 3 months. There were fewer ganglion cells in the peripheral retina of the rd1 retina compared to controls ($p < 0.05$).

Please cite this article in press as: Saha S et al. Changes in ganglion cells during retinal degeneration☆. Neuroscience (2016), http://dx.doi.org/10.1016/j.neuroscience.2016.04.032

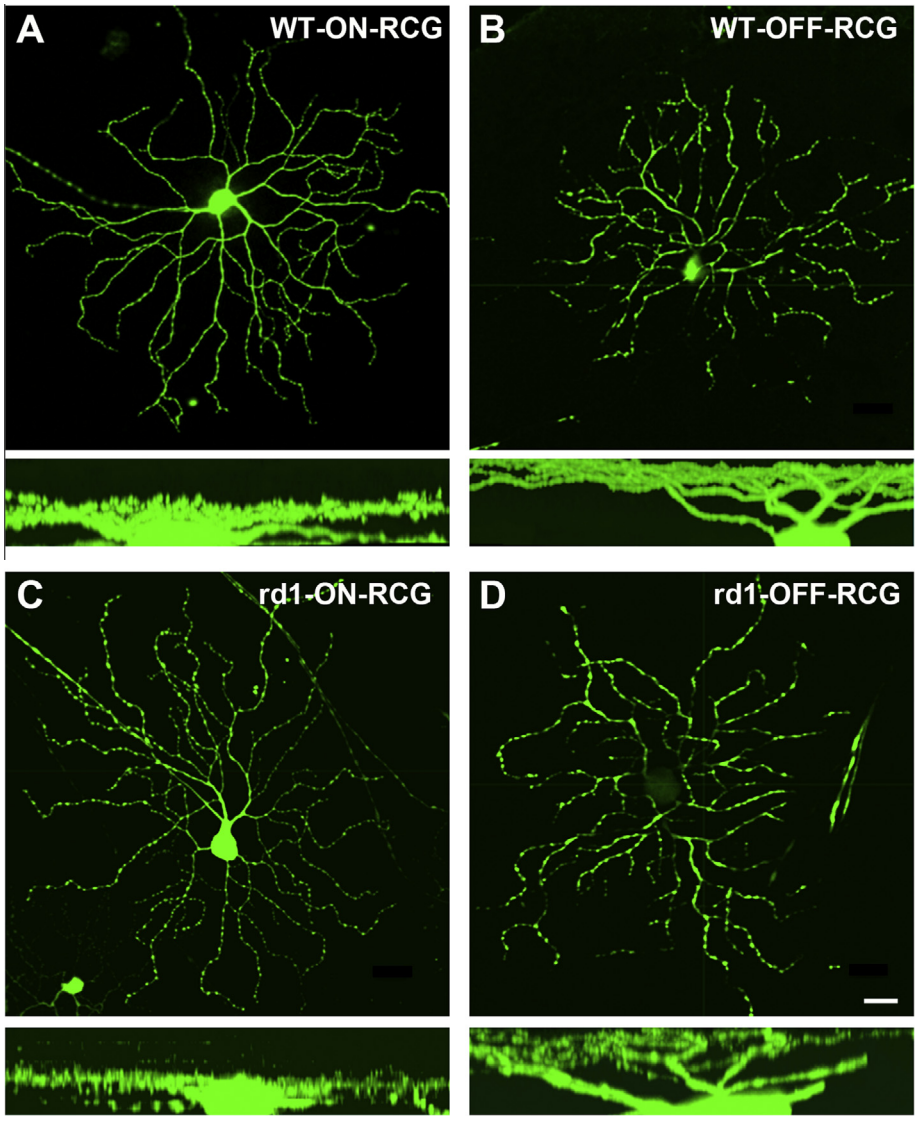

Fig. 3. ON and OFF ganglion cell identification in wildtype and rd retina. (A, B) Examples of a wildtype-ON RGC (soma and dendrites are in focus in the same plane) and a wildtype-OFF RGC (soma is not in focus) respectively. Beneath each image is a vertical section through the cell showing the stratification of processes through the IPL. (C, D) Examples of an rd1-ON RGC (soma and dendrites are in focus in the same plane) and an rd1-OFF RGC (soma is not in focus). Beneath each image are tilted images of *z*-scans showing the stratification of processes through the IPL; scale bar = 300 μm.

puncta labelling associated with OFF GCs (Fig. 4E) at one month of age. Moreover, there was a greater density of RIBEYE-immunoreactive puncta associated with ON ganglion cells compared to OFF ganglion cells ($p < 0.01$), and no difference in the density of gephyrin-immunoreactive puncta associated with ON or OFF ganglion cells (Fig. 4E). These results are consistent with a recent study by Soto et al. (2011) of ON and OFF ganglion cells in normal mouse retina. No significant change in synaptic density was observed in the wildtype retina for either synapse type between one and three months.

We next compared the density of excitatory and inhibitory synaptic puncta on ON A-ganglion cell processes of rd1-Thy1 compared to wildtype-Thy1, control retinae (Fig. 5A–C; wildtype, WT, white bars; rd1, gray bars). Quantitative analysis of synapses illustrated a significant decrease in RIBEYE-labeled ribbon synapse density associated with ON ganglion cells in rd1 retina at three months (Fig. 5A) and this was apparent for the entire length of a given dendrite (Fig. 5C). In contrast, there was no difference in the number of gephyrin-immunoreactive inhibitory puncta associated with ON ganglion cell dendrites in wildtype and rd1 retinae at either age examined (Fig. 5B). In addition, we considered whether there was localized loss of RIBEYE-immunoreactive puncta by quantifying the maximum distance between puncta in ON ganglion cells of control and rd1 retinae. The mean distance between neighboring RIBEYE puncta was similar in both rd1 and control retinae (rd1 = 2.17 ± 0.12 μm; control = 1.68 ± 0.23 μm; unpaired *t*-test $p = 0.364$ N = 6 cells for each strain). However, the average maximum distance between neighboring puncta was

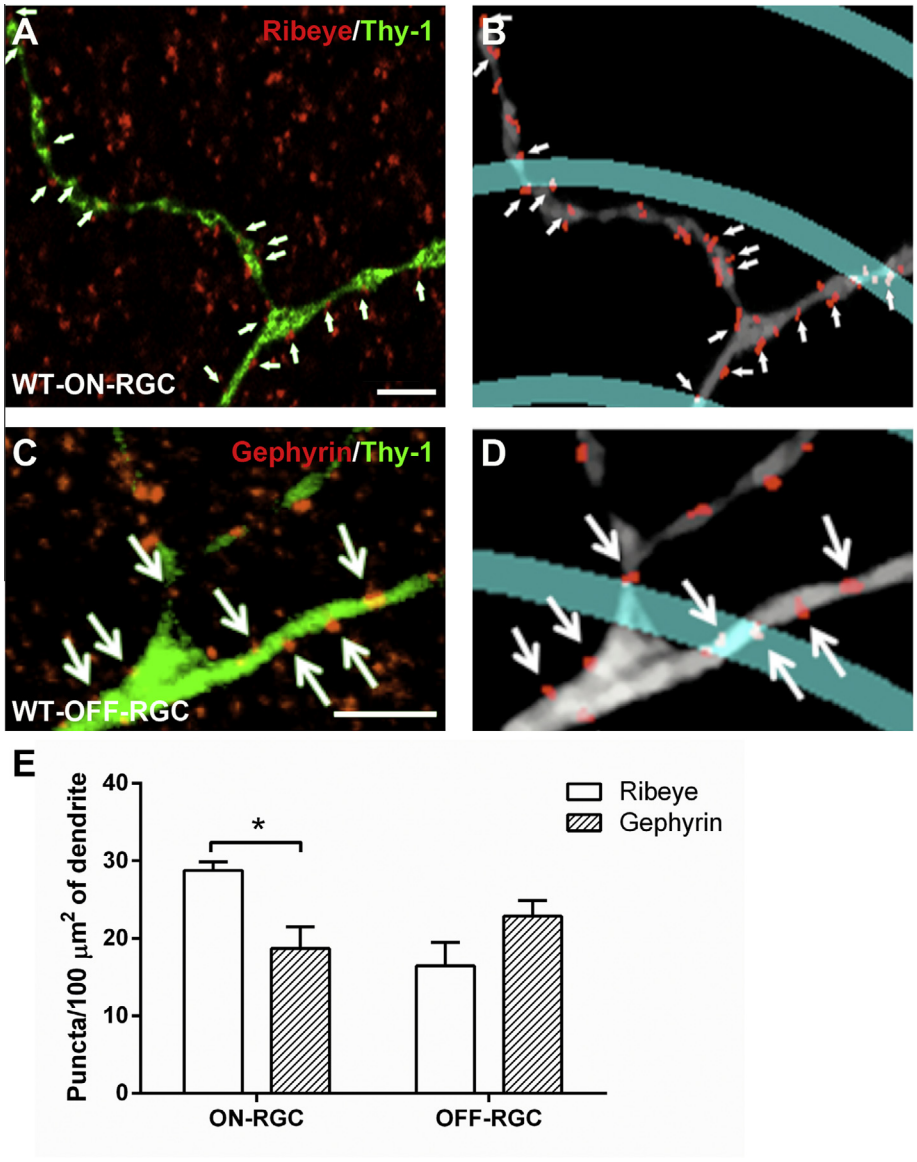

Fig. 4. Excitatory and inhibitory input to retinal ganglion cells differs between ON and OFF cells the wildtype mouse retina. Flatmount wildtype (C57bl/6J) retinae were immunolabeled for RIBEYE (A, red) and gephyrin (C, red) and Thy1-YFP-labeled ganglion cell processes (green). Both RIBEYE and gephyrin label small puncta many of which are associated (white arrows) with Thy1-YFP-labeled ganglion cell processes. These images were analyzed in Metamorph as shown in (B) RIBEYE, and (D) gephyrin, and red puncta associated with ganglion cell processes (white) were quantified. Scale bars in A & D = 10 μm. (E) Graph showing the number of RIBEYE and gephyrin-immunoreactive puncta per area of dendritic membrane for ON and OFF ganglion cells data presented as mean ± SEM. ON ganglion cells are associated with more RIBEYE-immunoreactive puncta than gephyrin puncta and there are more excitatory RIBEYE-immunoreactive pucta associated with ON than OFF RGCs (two-way ANOVA, $^{*}p < 0.05$). (For interpretation of the references to colour in this figure legend, the reader is referred to the web version of this article.)

significantly greater in rd1 retinae when compared to control retinae (14.84 ± 2.16 μm in rd1 and 8.918 ± 0.85 μm in control retinae; Mann–Whitney test, $p < 0.05$). Moreover, although puncta located at a distance greater than > 10um from their neighbor were rare, this occurred four times more frequently for rd1 (1.1%) than for control (0.25%) ON ganglion cells. Overall, these results suggest that following loss of photoreceptors there is a reduction in density of excitatory contacts associated with A-type ON ganglion cells and no change in inhibitory synapse density. Moreover, the loss of excitatory synaptic input may occur in localized regions, resulting in localized gaps in inputs.

Changes in excitatory and inhibitory synapses associated with OFF ganglion cells during degeneration

We next examined whether the density of RIBEYE or gephyrin-immunoreactive puncta was significantly altered in A-type OFF-ganglion cells during retinal degeneration. As shown in Fig. 5D-F, there was no difference between wildtype and rd1 in the density of

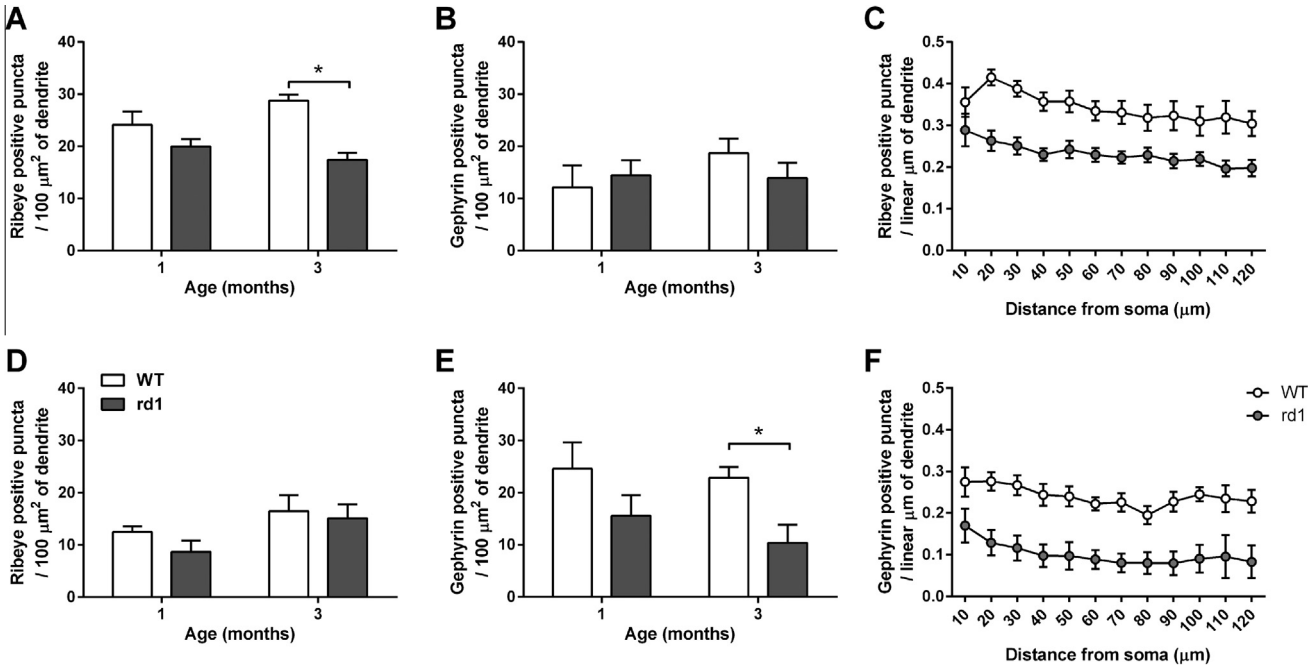

Fig. 5. Changes in RIBEYE and gephyrin association with ON (A–C) and OFF (D–F) ganglion cells in rd1 retinae. (A, B) Graphs showing mean ± SEM number of RIBEYE (A) and gephyrin (B) puncta associated with ON ganglion cells in wildtype (white bars) and rd1 (gray bars) retinae aged 1 and 3 months. The density of RIBEYE-immunoreactive puncta associated with ON ganglion cell is greater in rd1 retinae compared to wildtype at 3 months of age. The density of gephyrin associated with ON ganglion cells was no different in wildtype and rd1 retinae irrespective of age. (C) Graph showing the density of RIBEYE-immunoreactive puncta associated with ON ganglion cell processes at different locations within the dendritic tree. Although the density of RIBEYE was greater in widltype ON ganglion cells than rd1 retinae, there was no difference across the eccentricity of the dendrites. (D, E) Graphs show mean ± SEM number of RIBEYE (D) and gephyrin (E) puncta per area of dendritic membrane of OFF ganglion cells. The density of gephyrin associated with OFF ganglion cells was reduced in rd1 retinae at 3 months of age. (F) Graph showing the density of gephyrin puncta at different locations along the dendritic tree of OFF ganglion cells. Although the density of gephyrin was greater in wildtype OFF ganglion cells compared to rd1, there was no difference in density along the dendritic tree.

RIBEYE-immunoreactive, excitatory synapses associated with OFF ganglion cell dendrites irrespective of the age examined (Fig. 5D). However, we observed a significant reduction in inhibitory synapse density associated with rd1 OFF-ganglion cells at 3 months of age (Fig. 5E; Two-way ANOVA, $p < 0.05$). In addition, this reduction in gephyrin-immunoreactive puncta associated with OFF ganglion cells was apparent for the entire length of a given dendrite (Fig. 5F).

Rod and cone bipolar cell number is reduced in the rd1 compared to the wildtype retina

A possible explanation for the change in excitatory synapses associated with ON ganglion cells is the loss of bipolar cell inputs to ganglion cells. We examined whole mounted retinae to determine whether the change in excitatory synapse density could be explained by localized loss of immunolabeled sub-classes of bipolar cells and/or their terminals. As shown in Fig. 6A–D, there were gaps in tiling of the PKCα-labeled rod bipolar cell somata (Fig. 6A) and ZNP1-labeled cone bipolar cell somata (Type 6 ON-cone bipolar and Type 2 OFF-cone bipolar; Fig. 6B) as well as their axon terminals (Rod bipolars, Fig. 6C; Type 2-OFF cone bipolar terminals Fig. 6D), suggesting that there may be a localized change in expression of bipolar cell proteins or a loss of both rod and some cone bipolar cell subtypes at 3 months of degeneration in the rd1 retina. We then used immunocytochemistry on transverse sections to quantify ON bipolar cells in the rd1 compared to the control retina (Fig. 6E–H). We evaluated the number of PKC-immunoreactive rod bipolar cells across the retina (Fig. 6E, green) and also the number of Goα-positive bipolar cells (Fig. 6F, red), which is a marker of all depolarizing, rod and ON cone bipolar cells (Vardi, 1998). We then determined the number for Goα-positive /PKC-negative bipolar cells as a way of determining the density of ON cone bipolar cells (Fig. 6G; arrows indicate Goα-positive /PKC-negative bipolar cells). The total number of rod and ON cone bipolar cells in the inner nuclear layer was quantified in central and peripheral retina of wildtype and rd1 retina at 3 months of age (Fig. 6H). Overall, the density of rod bipolar and cone ON-bipolar cells was lower in rd1 retinae compared to control retinae (Rod Bipolar cells *t*-test $p < 0.01$; ON Cone Bipolar cells $p < 0.001$). These data are consistent with previous studies (Strettoi et al., 2002; Chen et al., 2012).

DISCUSSION

The major findings of this study were that following loss of photoreceptors in rd1 mice, excitatory synapses with A-type ON ganglion cells and inhibitory synapses with A-type OFF ganglion cells were reduced. The reduction in excitatory synapses with ON ganglions cells was

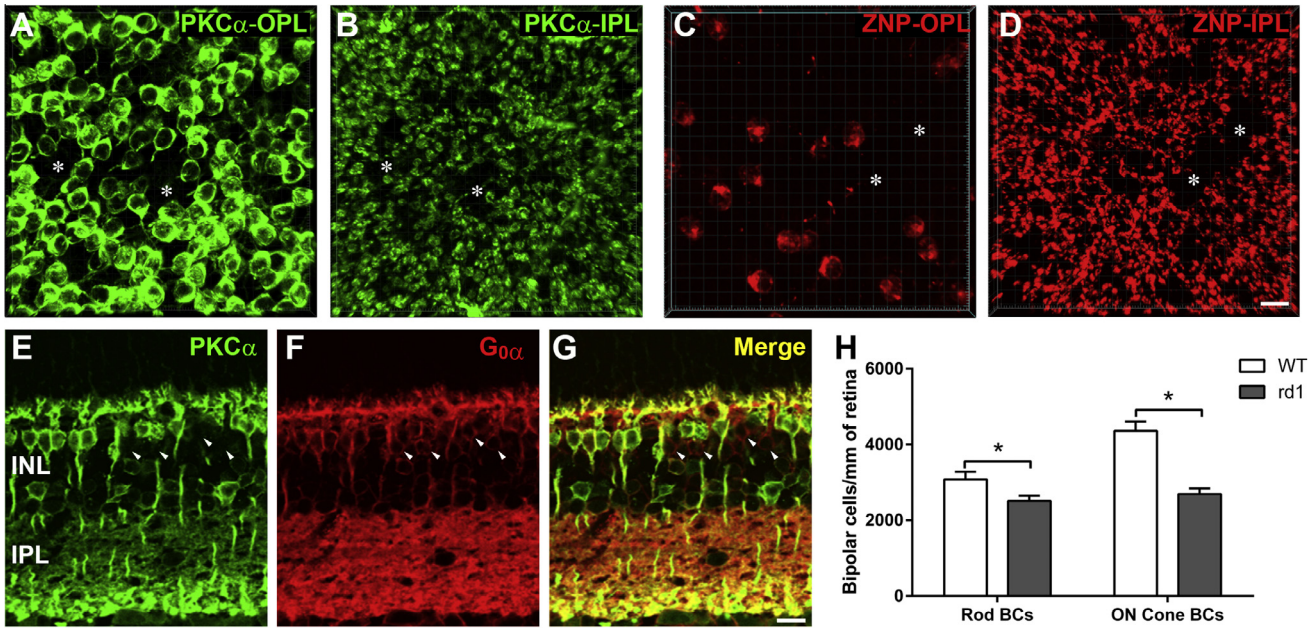

Fig. 6. Bipolar cells analysis in control and rd1 retinae. (A, B) Flatmount rd1 retinae immunolabeled for the rod bipolar cell marker, PKCα imaged at the level of somata close to the OPL (A) and the level of their axon terminals within S5 of the IPL (B). Gaps in the tiling of the retina were evident both at the level of the cell bodies (asterisks) and their axon terminals. (C, D) Flatmount rd1 retinae immunolabeled for the cone biplolar cell marker, ZNP imaged at the level of their cell bodies within the INL and their axon terminals within the OFF-sublaminae of the IPL. Gaps in the tiling of axon terminals and their somata were evident (asterisk). (E–G) Vertical sections of 3-month-old rd1 retinae double labeled for (E) PKCα green, (F) Goα, red and (G) merged. ON cone bipolar cells can be distinguished from rod bipolar cells by their labelling for Goα and their lack of PKCα labelling (white arrowheads). (H) Graph showing mean ± SEM density of rod bipolar cells and ON cone bipolar cells in control and rd1 retinae aged 3 months. The density of immunolabelled rod bipolar cells and ON cone bipolar cells was reduced in rd1 retinae compared to control retinae ($p < 0.05$). Scale bar for A–D, 10 μm. Scale bar for E–G = 10 μm. (OPL, outer plexiform layer; IPL, inner plexiform layer.) (For interpretation of the references to colour in this figure legend, the reader is referred to the web version of this article.)

associated with a reduction in rod bipolar cell and ON cone bipolar cell density. Overall, these findings indicate that as well as a small loss of retinal ganglion cells in the periphery of the rd1 retina at 3 months, there are significant alterations in the density of synaptic inputs to ganglion cells that could influence cellular function of the remaining ganglion cells in the rd1 retina.

In this study we identified ribbon synapses by immunocytochemically labeling for CtBP2 a ribbon-associated protein (Schmitz et al., 2000). Our results showed that the linear density of ribbon synapses presynaptic to A type ON ganglion cells was 0.39 puncta per μm, in close agreement with previous studies using alternative methods (Soto et al., 2011; Chen and Chiao, 2014). Inhibitory synapses were identified in this study by immunolabelling for gephyrin a clustering molecule that tethers glycine receptors and most $GABA_A$ receptors to the cytoskeleton (Tyagarajan and Fritschy, 2014). The results of this study show that the normal retina ON A type ganglion cells receive predominantly excitatory inputs (61% of synapses are CtBP2 immunoreactive) whereas OFF ganglion cells receive predominantly inhibitory inputs (~60% of inputs are gephyrin immunoreactive). The ratio of bipolar and amacrine cell inputs to ganglion cells is likely influenced by species, ganglion cell type and eccentricity. Using similar immunocytochemical methods, Percival et al. showed that excitatory and inhibitory input to ON and OFF ganglion cells were similar in the marmoset retina (Percival et al., 2009). In addition, Soto et al. (2011) used biolistic methods and showed that large field ON ganglion cells receive equal numbers of excitatory and inhibitory synapses (Soto et al., 2011; Chen and Chiao, 2014). It is not clear why our results are at subtle odds with these other studies. One possibility is that there are differences in the techniques used to label synapses between these studies. In the present study, immunohistochemical techniques would likely provide more variable labeling than genetic techniques (Soto et al., 2011). In the present study, puncta counts less than 10 microns from the soma were more variable between cells than those along the processes, which may have arisen from lesser spatial resolution of puncta when using immunohistochemistry. This may have contributed to the difference in findings when compared to the work of Soto et al., 2011. Another possibility is that gephyrin immunoreactivity used in this study under-estimated the number of inhibitory synapses. Inhibitory input to OFF ganglion cells is thought to be mediated predominantly via glycinergic receptors, whereas inhibitory inputs to ON ganglion are thought to be dominated by mechanisms involving GABA. Thus, gephyrin most likely identifies the full complement of inhibitory inputs to OFF ganglion cells, but could underestimate the extent of inhibitory input to ON ganglion cells.

Our results show that ganglion cell density is unchanged in the central rd1 retina at 3 months of age, but is reduced in the periphery. Several studies have shown that ganglion cell density remains largely intact

until very late stages of degeneration (Sekirnjak et al., 2009; Kolomiets et al., 2010; Damiani et al., 2012; Lin and Peng, 2013), however these studies did not investigate retinal eccentricity. The underlying mechanism for loss of ganglion cells in the peripheral retina in the three-month-old rd1 mouse is not clear. Previous studies indicate that when ganglion cell loss is observed it is associated with the most advanced stages of retinal degeneration, perhaps reflecting a response to the gross anatomical changes that are known to occur in the inner retina at late stages of degeneration (Sekirnjak et al., 2009; Kolomiets et al., 2010; Damiani et al., 2012). More work is required to elucidate more clearly the underlying mechanism(s) for ganglion cell loss in retinal degeneration.

We observed a reduction in the number of excitatory synapses associated with ON ganglion cells from rd1 retinae aged 3 months compared to control retinae. In addition, there was a reduction in Goα-labeled ON cone bipolar cells at a concomitant stage of degeneration. These data may indicate a reduction in Goα-immunoreactivity in ON cone bipolar cells as has been seen for mGluR6 in the rd10 mouse (Puthussery et al., 2009) or a reduction in the number of ON cone bipolar cells. A loss of ON cone bipolar cells would be consistent with the results of Chen et al. (2012), who demonstrated a progressive reduction in synaptic ribbons in type 7 ON cone bipolar cells from 3 to 12 months of age in rd1 retinae and also Strettoi et al. (2002, 2003) and Ogilvie et al. (1997) who demonstrated morphological changes and a reduction in both rod and subsets of cone bipolar cells in the rd1 retina. It is known that rd1 mice have a developmental anomaly involving a failure of development of invaginating synapses between photoreceptor and bipolar cells (Blanks et al., 1974). However, unlike rod bipolar cells, cone ON and OFF bipolar cells succeed in reaching maturity in rd1 mice, with retraction of dendrites in the OPL only occurring following cone death (Strettoi et al., 2002, 2003). Thus, abnormal development and/or abnormal function of ON bipolar cells could be implicated in the reduced density of excitatory inputs to ON ganglion cells. Alternatively, there may be sporadic, random death of bipolar cells as retinal degeneration proceeds. Indeed, we observed small gaps in the tiling of rod bipolar cell somata and their axon terminals possibly reflecting changes in cellular expression of proteins or a loss of a small number of cells.

In this study we observed a reduction in the density of gephyrin-immunoreactive inputs to OFF ganglion cells, suggesting reduced inhibitory input to these cells. Shifts in gephyrin clustering has been reported in response to changes in neural inputs. It is thought that neural activity triggers mobilization of glycine receptors to the synaptic membrane via calcium-dependent transport mechanisms (Tyagarajan and Fritschy, 2014). It is well known that ganglion cells, especially OFF ganglion cells, are functionally altered from an early age in the rd1 retina (Stasheff, 2008). It is possible that the reduction in synaptic inputs via gephyrin-clustered glycine or GABA receptors could be associated with these functional alterations. In contrast, to the changes in inhibitory inputs, there were no changes in excitatory input to OFF A-type ganglion cells, despite some evidence of loss of Type 2 OFF cone bipolar cell terminals at three months (Fig. 6D). This suggests either that OFF A-type ganglion cells do not receive synaptic input from Type 2 OFF cone bipolar cells or that the loss of these inputs is very infrequent and does not contribute greatly to the excitatory compliment received by OFF A-type ganglion cells.

The observation that there are alterations in the density of excitatory and inhibitory synapses on ON and OFF ganglion cells during degeneration has implications for vision restoration especially those methods involving direct electrical (Sekirnjak et al., 2006) or optical stimulation (Farah et al., 2007). Vision restoration is currently possible in those with advanced forms of retinal degeneration, at a comparable, or even more advanced stage than the current study. In particular, with the altered density of excitatory and inhibitory inputs expressed by ON and OFF ganglion cells, electrical stimulation could affect ON and OFF ganglion cells in different ways. Further studies are required to explore the impact that altered function of ON and OFF ganglion cells has on vision restoration and whether these differences could be exploited to target either the ON or OFF pathway specifically.

In summary, the results of this study have demonstrated that there are alterations in the density and spatial distribution of excitatory and inhibitory synapses with ON and OFF ganglion cells well after photoreceptor loss. In agreement with these findings, we also observed a reduction in density of rod bipolar and ON cone bipolar cells. These findings could at least partially explain the aberrant electrophysiological function previously reported in ON ganglion cells during degeneration. In addition, the results shown could have implications in the optimization of photoreceptor restoration therapies. The mechanism by which these changes occur, however, remain to be determined.

REFERENCES

Blanks JC, Adinolfi AM, Lolley RN (1974) Photoreceptor degeneration and synaptogenesis in retinal-degenerative (rd) mice. J Comp Neurol 156:95–106.

Chader GJ, Weiland J, Humayun MS (2009) Artificial vision: needs, functioning, and testing of a retinal electronic prosthesis. Prog Brain Res 175:317–332.

Chen M, Wang K, Lin B (2012) Development and degeneration of cone bipolar cells are independent of cone photoreceptors in a mouse model of retinitis pigmentosa. PLoS ONE 7.

Chen YP, Chiao CC (2014) Spatial distribution of excitatory synapses on the dendrites of ganglion cells in the mouse retina. PLoS ONE 9:e86159.

Damiani D, Novelli E, Mazzoni F, Strettoi E (2012) Undersized dendritic arborizations in retinal ganglion cells of the rd1 mutant mouse: a paradigm of early onset photoreceptor degeneration. J Comp Neurol 520:1406–1423.

Erikoz B, Jusuf PR, Percival KA, Grunert U (2008) Distribution of bipolar input to midget and parasol ganglion cells in marmoset retina. Vis Neurosci 25:67–76.

Famiglietti EV, Kolb H (1976) Structural basis for On-center and OFF-center responses in retinal ganglion cells. Science 194:193–195.

Farah N, Reutsky I, Shoham S (2007) Patterned optical activation of retinal ganglion cells. Conference Proceedings: Annual

International Conference of The IEEE Engineering In Medicine And Biology Society IEEE Engineering In Medicine And Biology Society Annual Conference 2007:6368–6370.
Feng G, Mellor RH, Bernstein M, Keller-Peck C, Nguyen QT, Wallace M, Nerbonne JM, Lichtman JW, Sanes JR (2000) Imaging neuronal subsets in transgenic mice expressing multiple spectral variants of GFP. Neuron 28:41–51.
Fletcher EL (2000) Alterations in neurochemistry during retinal degeneration. Microsc Res Tech 50:89–102.
Freed MA, Sterling P (1988) The ON-alpha ganglion cell of the cat retina and its presynaptic cell types. J Neurosci 8:2303–2320.
Greferath U, Grunert U, Wässle H (1990) Rod bipolar cells in the mammalian retina show protein kinase C-like immunoreactivity. J Comp Neurol 301:433–442.
Haverkamp S, Wässle H (2000) Immunocytochemical analysis of the mouse retina. J Comp Neurol 424:1–23.
Ho T, Vessey KA, Cappai R, Dinet V, Mascarelli F, Ciccotosto GD, Fletcher EL (2012) Amyloid precursor protein is required for normal function of the rod and cone pathways in the mouse retina. PLoS ONE 7:e29892.
Humayun MS, Prince M, de Juan E, Barron Y, Moskowitz M, Klock IB, Milam AH (1999) Morphometric analysis of the extramacular retina from postmortem eyes with retinitis pigmentosa. Invest Ophthalmol Vis Sci 40:143–148.
Jakobs TC, Koizumi A, Masland RH (2008) The spatial distribution of glutamatergic inputs to dendrites of retinal ganglion cells. J Comp Neurol 510:221–236.
Koizumi A, Jakobs TC, Masland RH (2011) Regular mosaic of synaptic contacts among three retinal neurons. J Comp Neurol 519:341–357.
Kolomiets B, Dubus E, Simonutti M, Rosolen S, Sahel JA, Picaud S (2010) Late histological and functional changes in the P23H rat retina after photoreceptor loss. Neurobiol Dis 38:47–58.
Koulen P, Sassoe-Pognetto M, Grunert U, Wässle H (1996) Selective clustering of GABA(A) and glycine receptors in the mammalian retina. J Neurosci 16:2127–2140.
Lin B, Peng EB (2013) Retinal ganglion cells are resistant to photoreceptor loss in retinal degeneration. PLoS ONE 8:e68084.
Marc RE, Jones BW, Watt CB, Strettoi E (2003) Neural remodeling in retinal degeneration. Prog Retin Eye Res 22:607–655.
Margolis DJ, Newkirk G, Euler T, Detwiler PB (2008) Functional stability of retinal ganglion cells after degeneration-induced changes in synaptic input. J Neurosci 28:6526–6536.
O'Brien EE, Greferath U, Fletcher EL (2014) The effect of photoreceptor degeneration on ganglion cell morphology. J Comp Neurol 522:1155–1170.
O'Brien EE, Greferath U, Vessey KA, Jobling AI, Fletcher EL (2012) Electronic restoration of vision in those with photoreceptor degenerations. Clin Exp Optom 95:473–483.
Ogilvie JM, Tenkova T, Lett JM, Speck J, Landgraf M, Silverman MS (1997) Age-related distribution of cones and ON-bipolar cells in the rd mouse retina. Curr Eye Res 16:244–251.
Percival KA, Jusuf PR, Martin PR, Grunert U (2009) Synaptic inputs onto small bistratified (blue-ON/yellow-OFF) ganglion cells in marmoset retina. J Comp Neurol 517:655–669.
Percival KA, Martin PR, Grunert U (2011) Synaptic inputs to two types of koniocellular pathway ganglion cells in marmoset retina. J Comp Neurol 519:2135–2153.
Percival KA, Martin PR, Grunert U (2013) Organisation of koniocellular-projecting ganglion cells and diffuse bipolar cells in the primate fovea. Eur J Neurosci 37:1072–1089.
Puthussery T, Gayet-Primo J, Pandey S, Duvoisin RM, Taylor WR (2009) Differential loss and preservation of glutamate receptor function in bipolar cells in the rd10 mouse model of retinitis pigmentosa. Eur J Neurosci 29:1533–1542.
Rodriguez AR, de Sevilla Müller LP, Brecha NC (2014) The RNA binding protein RBPMS is a selective marker of ganglion cells in the mammalian retina. J Comp Neurol 522:1411–1443.
Santos A, Humayun MS, deJuan E, Greenburg RJ, Marsh MJ, Klock IB, Milam AH (1997) Preservation of the inner retina in retinitis pigmentosa – a morphometric analysis. Arch Ophthalmol 115:511–515.
Schmitz F, Konigstorfer A, Sudhof TC (2000) RIBEYE, a component of synaptic ribbons: a protein's journey through evolution provides insight into synaptic ribbon function. Neuron 28:857–872.
Sekirnjak C, Hottowy P, Sher A, Dabrowski W, Litke AM, Chichilnisky EJ (2006) Electrical stimulation of mammalian retinal ganglion cells with multielectrode arrays. J Neurophysiol 95:3311–3327.
Sekirnjak C, Hulse C, Jepson LH, Hottowy P, Sher A, Dabrowski W, Litke AM, Chichilnisky EJ (2009) Loss of responses to visual but not electrical stimulation in ganglion cells of rats with severe photoreceptor degeneration. J Neurophysiol 102:3260–3269.
Sekirnjak C, Jepson LH, Hottowy P, Sher A, Dabrowski W, Litke AM, Chichilnisky EJ (2011) Changes in physiological properties of rat ganglion cells during retinal degeneration. J Neurophysiol 105:2560–2571.
Soto F, Bleckert A, Lewis R, Kang Y, Kerschensteiner D, Craig AM, Wong RO (2011) Coordinated increase in inhibitory and excitatory synapses onto retinal ganglion cells during development. Neural Dev 6:31.
Stasheff SF (2008) Emergence of sustained spontaneous hyperactivity and temporary preservation of OFF responses in ganglion cells of the retinal degeneration (rd1) mouse. J Neurophysiol 99:1408–1421.
Stasheff SF, Shankar M, Andrews MP (2011) Developmental time course distinguishes changes in spontaneous and light-evoked retinal ganglion cell activity in rd1 and rd10 mice. J Neurophysiol 105:3002–3009.
Strettoi E, Pignatelli V (2000) Modifications of retinal neurons in a mouse model of retinitis pigmentosa. Proc Natl Acad Sci U S A 97:11020–11025.
Strettoi E, Pignatelli V, Rossi C, Porciatti V, Falsini B (2003) Remodeling of second-order neurons in the retina of rd/rd mutant mice. Vision Res 43:867–877.
Strettoi E, Porciatti V, Falsini B, Pignatelli V, Rossi C (2002) Morphological and functional abnormalities in the inner retina of the rd/rd mouse. J Neurosci 22:5492–5504.
Sun WZ, Li N, He SG (2002) Large-scale morphological survey of mouse retinal ganglion cells. J Comp Neurol 451:115–126.
Tyagarajan SK, Fritschy JM (2014) Gephyrin: a master regulator of neuronal function? Nat Rev Neurosci 15:141–156.
Vardi N (1998) Alpha subunit of Go localizes in the dendritic tips of ON bipolar cells. J Comp Neurol 395:43–52.
Vessey KA, Fletcher EL (2012) Rod and cone pathway signalling is altered in the P2X7 receptor knock out mouse. PLoS ONE 7: e29990.
Wässle H, Puller C, Müller F, Haverkamp S (2009) Cone contacts, mosaics, and territories of bipolar cells in the mouse retina. J Neurosci 29:106–117.
Wässle H, Yamashita M, Greferath U, Grunert U, Müller F (1991) The rod bipolar cell of the mammalian retina. Vis Neurosci 7:99–112.
Xu Y, Vasudeva V, Vardi N, Sterling P, Freed MA (2008) Different types of ganglion cell share a synaptic pattern. J Comp Neurol 507:1871–1878.

(Accepted 21 April 2016)
(Available online xxxx)